Available online at www.sciencedirect.com
SCIENCE DIRECT®
Precambrian Research 144 (2006) 1–18
Precambrian Research
www.elsevier.com/locate/precamres

Zircon SHRIMP U–Pb dating, C and O isotopes for impure marbles from the Jiaobei terrane in the Sulu orogen: Implication for tectonic affinity

Jun Tang [a,b], Yong-Fei Zheng [a,*], Yuan-Bao Wu [a], Bing Gong [a]

[a] CAS Key Laboratory of Crust-Mantle Materials and Environments, School of Earth and Space Sciences, University of Science and Technology of China, Hefei 230026, China
[b] Beijing SHRIMP Center, Chinese Academy of Geological Sciences, Beijing 100037, China

Received 24 January 2005; received in revised form 9 September 2005; accepted 1 October 2005

Abstract

Middle Neoproterozoic carbonates are found in the western part of Shandong Pennisula (i.e., the Jiaobei terrane) that is located in the northwestern part of the Sulu orogen in east-central China. For the first time, a successful SHRIMP U–Pb dating, coupled with CL imaging, was conducted on two samples of impure marble from the Fenzishan Group in this tectonic unit. The results yield consistent ages of 786 ± 67 and 240 ± 44 Ma for igneous and metamorphic zircons, respectively. Positive $\delta^{13}C$ values as high as +5.6‰ are measured for both pure and impure marbles, consistent not only with the worldwide Neoproterozoic limestones in connection with the Sturtian ice-age, but also with the marbles associated with UHP metamorphic eclogites in the Dabie orogen. O isotope fractionation between calcite and garnet from one sample gave a temperature of 680 °C, pointing to upper amphibolite-facies metamorphic conditions. These results indicate that protolith of the marbles is a kind of limestone that was synchronously deposited with volcaniclastic rocks in the mid-Neoproterozoic rift basin of continental margin. Like the UHP metamorphic rocks in the Dabie-Sulu orogenic belt, both mid-Neoproterozoic magmatism and Triassic metamorphism are recorded in the impure marbles. Therefore, protolith of the impure marbles corresponds to the sedimentary limestone of rift basin developed during the mid-Neoproterozoic breakup of supercontinent Rodinia, but it was the sedimentary cover along the northern margin of the South China Block prior to its Triassic subduction. The occurrence of the mid-Neoproterozoic limestone with the Triassic metamorphism in the southern margin of the North China Block thus indicates tectonic overthrust by a crustal detachment between the sedimentary cover and the Precambrian basement during the continent subduction. As a result, the marbles in affinity to the South China Block were northward thrusted over the basement of the North China Block.

Keywords: Neoproterozoic limestone; Triassic metamorphism; Continent subduction; Tectonic overthrust; Crustal detachment

1. Introduction

Since the first successful Pb–Pb dating of stromatolitic limestone by Moorbath et al. (1987), many attempts to date carbonate rocks of Archean to Mesozoic ages by the Pb–Pb and U–Pb isochron methods have yielded significant results (Moorbath et al., 1987; Jahn, 1988; Jahn et al., 1990; Taylor and Kalsbeek, 1990;

* Corresponding author. Tel.: +86 55 13603554;
fax: +86 55 13603554.
E-mail address: yfzheng@ustc.edu.cn (Y.-F. Zheng).

0301-9268/$ – see front matter © 2005 Elsevier B.V. All rights reserved.
doi:10.1016/j.precamres.2005.10.003

Jahn and Cuvellier, 1994; Woodhead and Hergt, 1997; Wang et al., 1998; Fölling et al., 2000). Despite relatively large age uncertainties compared to zircon dating, the application of carbonate Pb–Pb and U–Pb chronology has made an important contribution to the dating of primary deposition of limestone or metamorphism of marble. The validity of carbonate U–Pb and Pb–Pb ages rests upon the close-system behavior of U and Pb. Since the U–Pb isotopic system in carbonate rocks sometimes can be disturbed during diagenesis or retrograde metamorphism, the aberrant ages have been obtained occasionally. Therefore, the carbonate U–Pb or Pb–Pb ages alone do not always provide a definite geological meaning, thus a multi-chronometric approach has to be taken for any critical age determination (Jahn and Cuvellier, 1994).

Impure carbonate rocks sometimes contain detrital zircons which deposit synchronously with carbonate rocks. Because the behavior of U and Pb in zircon is more inert than that in carbonate rock, the U–Pb dating on the detrital zircons can provide reliable geochronological constrains on the deposition timing for impure carbonate rocks. Furthermore, the detrital zircons could experience recrystallization or overgrowth when the impure carbonate rocks underwent high-grade metamorphism, the U–Pb dating on such metamorphic zircons can provide metamorphic age for impure marble. On the other hand, C isotope composition of sedimentary and metamorphic carbonates can be used to reconstruct their deposition environments and tectonic affinity if no significant water–rock interaction has altered their original signatures. In this study, a combination of the above two approaches is attempted for the case of impure marbles from the western part of Shandong Pennisula (i.e., the Jiaobei terrane) in the Sulu orogen, east-central China. The results provide insight not only into their protolith nature and metamorphic event in a collisional orogenic belt, but also into tectonic overthrust by a crustal detachment between cover and basement during continent subduction.

2. Geological settings and samples

The Jiaobei terrane is bounded to the northwest by the Tanlu fault, to the south by the Jiaolai Basin, and to the southeast by the Wulian-Yantai fault that marks the northern margin of the ultrahigh-pressure (UHP) metamorphic zone in the Sulu orogen (Fig. 1a). It mainly consists of Precambrian basement (TTG gneisses and metasedimentary covers) as well as Mesozoic granitoids and volcanics (Fig. 1b). The metasedimentary covers are categorized into two sequences, the Paleoproterozoic Fenzishan Group and the Neoproterozoic Penglai Group (Faure et al., 2003). However, the precise location for the Wulian-Yantai fault in the middle part of the Shandong Peninsula is controversial due to the intensive overprint by the Mesozoic tectono-magmatism (Wallis et al., 1999; Zhai et al., 2000). A great deal of tectonic, petrological and geochronological studies have demonstrated that protolith of the UHP metamorphic rocks in the Sulu orogen is responsible for igneous and sedimentary rocks in the northern margin of the South China

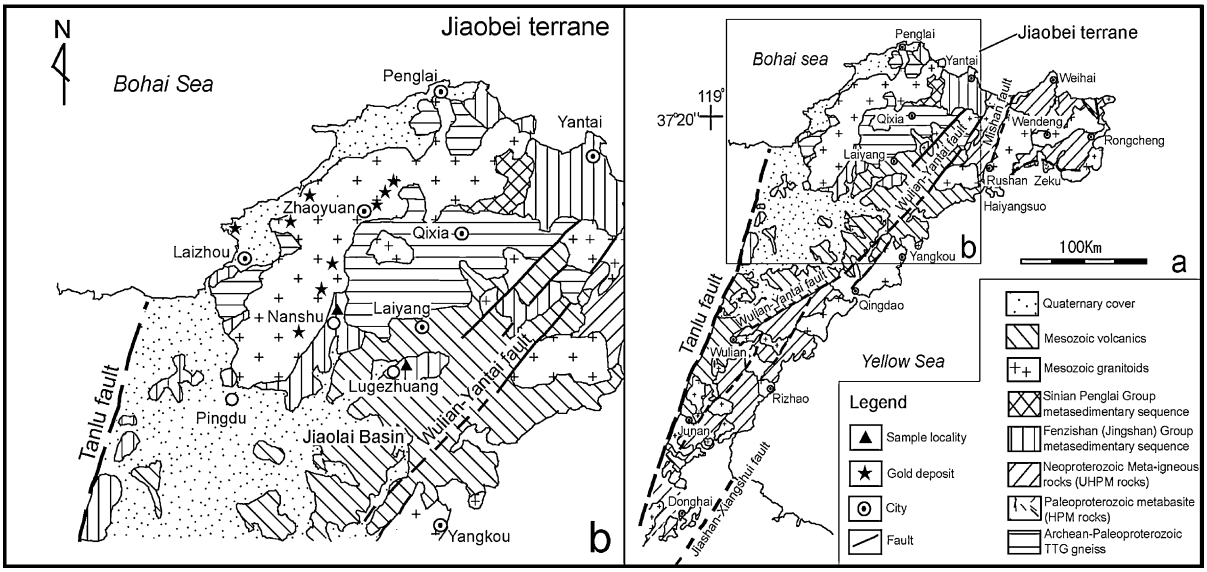

Fig. 1. Sketch geological map of the Sulu orogen in the Shandong Peninsula (a) and the Jiaobei terrane (b) with sample locality.

Block (SCB), with middle Neoproterozoic ages for the protolith of UHP metaigneous rocks (Zheng et al., 2003, 2004, 2005). Triassic UHP metamorphic event has been well established for both metaigneous and metasedimentary rocks in the Dabie-Sulu orogenic belt (Ames et al., 1996; Hacker et al., 1998; Li et al., 1999; Zheng et al., 2003). Early Cretaceous magmatism of ultramafic to felsic compositions is also recognized in this orogenic belt (Cong, 1996; Liou et al., 1996; Zhao et al., 2004, 2005).

The Precambrian basement in Jiaobei mainly consists of Neoarchean-Paleoproterozoic TTG gneisses, Paleoproterozoic Fenzishan Group and Neoproterozoic (Nanhua-Sinian) Penglai Group. The TTG gneisses are situated in the center region of Jiaobei terrane. Protolith of the TTG gneisses are dated by the TIMS zircon U–Pb methods to be emplaced at 1.9–2.7 Ga (Wang and An, 1996; Lu, 1998), while their metamorphic timing of amphibolite-facies to granulite-facies is about 1.7–1.8 Ga in terms of Sm–Nd and Ar–Ar dating (Zhai et al., 2000; Faure et al., 2003). Therefore, the Jiaobei terrane geotectonically belongs to the southern edge of the North China Block (NCB) that is characterized by the absence of mid-Neopproterozoic igneous rocks (Hacker et al., 1998; Wan and Zeng, 2002; Wu et al., 2004).

The Fenzishan Group, which is distributed in the southern and northern peripheries of Jiaobei terrane, uncomformably lies on the TTG gneisses. It mainly consists of paragneisses, schists, amphibolites and marbles. The sedimentary environments for the Fenzishan Group are littoral facies to shallow-sea facies with several volcanic cycles (An, 1990; Wang, 1995). Metamorphic grade of the Fenzishan Group in southern Jiaobei is upper amphibolite-facies to granulite-facies, while that in northern Jiaobei is upper greenschist-facies to lower amphibolite-facies (Wang and An, 1996; Zhou et al., 2001, 2004b). The Penglai Group also uncomformably lies on the TTG gneisses or the Fenzishan Group, and it mainly consists of crystalline limestones, slates and quartzites that only experienced lower greenschist-facies deformation-metamorphism (Faure et al., 2001, 2003).

The Fenzishan Group in the Nanshu and Lugezhuang areas is composed of sillimanite-garnet-bearing biotite schists, sillimanite-garnet-bearing biotite paragneisses, garnet-cordierite paragneisses, and marbles. The marble layers that are 300–500 m in thickness were subjected to intensive deformation and were locally truncated by faults (Shandong, 1991). The marbles are located northeast of the Wulian-Yantai fault in tens of kilometers (Fig. 1) and occur as both pure and impure ones in these two areas that are normally classified as the Zhanggezhuang Formation of the Fenzishan Group (equivalent to the Lugezhuang Formation of the Jinshan Group) (Wang, 1995).

Carbonate minerals in the pure marbles are calcite and dolomite, with calcite content exceeding 80%. The impure marbles contain variable amount of silicate minerals which include olivine, clinopyroxene, garnet, muscovite and serpentine (Fig. 2), with minor amounts of zircon, magnetite, pyrite and pyrrhotite. The mineral contents in marbles are listed in Table 1. Microscope observations indicate that the silicate minerals are basically of metamorphic genesis (Fig. 2). The olivine occurs in two forms, one is the granular crystal that has almost replaced by serpentine (Fig. 2a), and the other is the banded aggregate that underwent relatively weak serpentinization (Fig. 2b). Relicts of clinopyroxene and garnet occur sporadically (Fig. 2c–e). The muscovite only occurs in the secondary form along the margin of clinopyroxene as a result of retrograde metamorphism, and the undulatory extinction and curved cleavage plane suggest that the marbles were once subjected to intensive compression and deformation (Fig. 2d and e). The

Table 1
Mineral content (wt.%) for marbles from the Jiaobei terrane in the Sulu orogen

Sample number	Rock type	Locality	Cc	Dol	Ol	Cpx	Gt	Mus	Mt	Py	Pyr
02SD06[a]	Marble	Nanshu	80–85	15–20							
02SD07[b]	Impure marble	Nanshu	36	34	27	<1	4	<1			
02SD08[a]	Marble	Nanshu	80–85	15–20							
04SD07[b]	Impure marble	Nanshu	48	5	40	<1	2	2			<1
04SD08[a]	Olivine aggregate	Nanshu			90–95				5–10	1–3	
04SD11[a]	Impure marble	Nanshu	55–60	1–5	25–30	1–3	<1	1–3			
02SD16[b]	Impure marble	Lugezhuang	41	26	28	<1	3				
02SD17[a]	Marble	Lugezhuang	80–85	15–20							

Abbreviations: Cc, calcite; Cpx, clinopyroxene; Dol, dolomite; Gt, garnet; Mus, muscovite; Mt, magnetite; Py, pyrite; Pyr, pyrrhotite; Ol, olivine.
[a] Content estimated in thin section.
[b] Content calculated by CIPW method (relevant major element oxides are listed in Table 2) in following procedures: (1) K_2O is partitioned into Mus ($2K_2O·8Al_2O_3·8SiO_2·H_2O$); (2) excess Al_2O_3 is partitioned into Gt ($3CaO·Al_2O_3·3SiO_2$); (3) excess SiO_2 is partitioned into Ol ($2MgO·SiO_2$); (4) excess MgO is partitioned into Dol ($CaO·MgO·2CO_2$); (5) excess CaO is partitioned into Cc ($CaO·CO_2$).

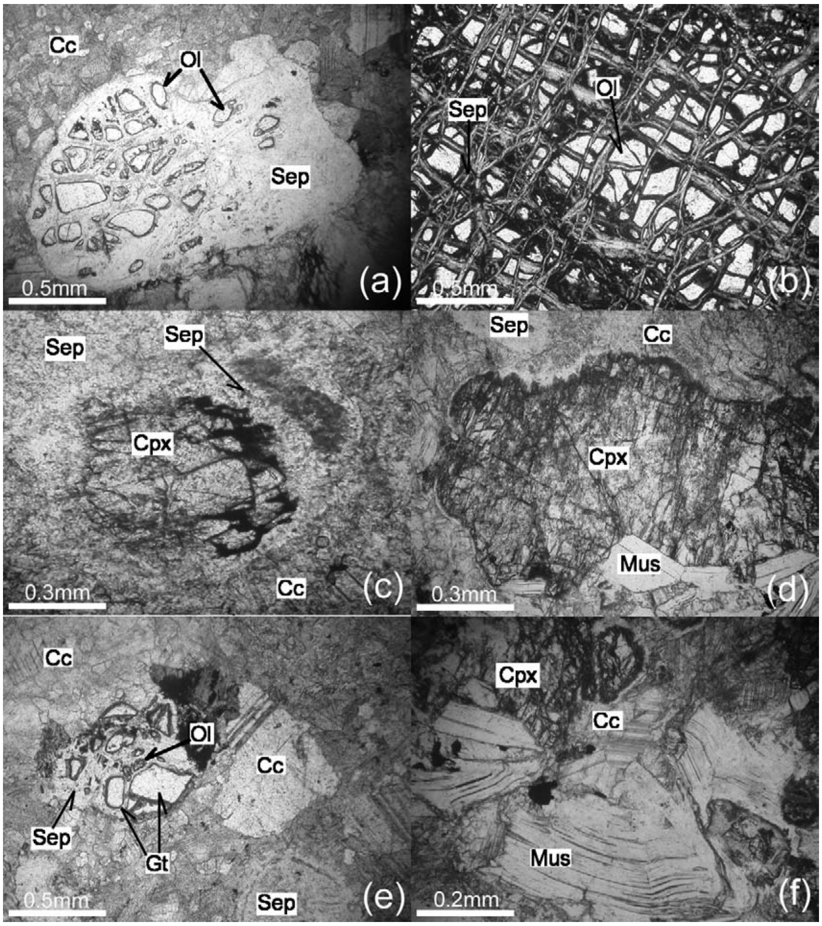

Fig. 2. Photomicrograph (polarized light) of impure marble at Nanshu in the Jiaobei terrane. (a) Sample 02SD07: serpentine pseudomorph after olivine which occurred as granular crystal in the impure marbles. (b) Sample 04SD08: cataclastic texture within banded olivine aggregate, serpentine occurred only along the cracks in olivine aggregate. (c) Sample 02SD07: clinopyroxene relict with cleavage that occurred as granular crystal in the impure marbles and surrounded by secondary serpentine. (d) Sample 04SD07: clinopyroxene relict with cleavage that occurred as granular crystal in the impure marbles and was replaced by muscovite in the margin, suggesting fluid activity during retrograde metamorphism. (e) Sample 02SD07: relicts of garnet and olivine within serpentine. (f) Sample 02SD07: muscovite that replaced clinopyroxene in the margin has curved plane of cleavage and undulatory extinction, suggesting intensive deformation. Abbreviations: Cc, calcite; Cpx, clinopyroxene; Gt, garnet; Mus, muscovite; Ol, olivine; Sep, serpentine.

micro-texture characteristics of the impure marbles in question are shown in Fig. 2.

3. Analytical methods

Mineral separation was conducted at Institute of Geochemical and Geophysical Prospecting of Hebei province at Langfang city, by using a combination of magnetic, heavy liquid, and hand-picking techniques which ensure the separate purity better than 98%. The zircons were picked up under binocular microscope for cathodoluminescence (CL) imaging and U–Pb dating. They are colorless, transparent, and have no fracture and mineral inclusion. Whole-rock powder (200 meshes) of marbles for major and trace element, C and O isotope analyses is processed in agate mortars in order to minimize potential contamination.

Major element oxides and trace elements analyses were carried out at the Guangzhou Institute of Geochemistry, using a Varian Vista PRO ICP-AES for major element oxides and a Perkin-Elmer Sciex ELAN 6000 ICP-MS for trace elements. Analytical procedures for major element analysis using ICP-AES are similar to those described by Ramsey et al. (1995), and the analytical precisions for major element oxides are better than 1–2% (Li et al., 2003). Analytical procedures for trace element analysis using ICP-MS are similar to those described by Li (1997), and the analytical precisions for

Table 2
Major and trace element compositions for impure marbles from the Jiaobei terrane in the Sulu orogen

Sample number	02SD07		02SD16		04SD07	
Rock type	Whole-rock	Silicates	Whole-rock	Silicates	Whole-rock	Silicates
SiO_2	13.11	42.37	13.10	41.93	17.63	41.07
TiO_2	0.02	0.06	0.01	0.03	0.03	0.07
Al_2O_3	0.93	3.01	0.71	2.27	1.58	3.68
Fe_2O_3	0.01	0.03	0.44	1.41	0.62	1.44
FeO	Trace		Trace		Trace	
MnO	0.01	0.03	0.01	0.03	0.01	0.02
MgO	22.67	49.42	21.46	50.55	23.21	51.45
CaO	30.32	4.95	30.77	3.74	29.06	1.57
Na_2O	0.03	0.10	0.00	0.00	0.03	0.07
K_2O	0.00	0.00	0.00	0.00	0.25	0.58
P_2O_5	0.01	0.03	0.01	0.03	0.02	0.05
L.O.I.	32.78		33.86		27.68	
Total	99.87	100.00	100.37	100.00	100.12	100.00
Trace element (ppm)						
Cs	0.026		0.035		0.532	
Rb	0.241		0.236		7.961	
Ba	65.16		183.5		56.87	
Th	0.454		0.646		7.089	
U	0.166		0.183		0.997	
Nb	0.133		0.034		1.138	
Ta	0.011		0.002		0.074	
Sr	129.5		101.1		182.4	
P	43.66		43.66		87.32	
Zr	7.84		1.478		6.921	
Hf	0.255		0.042		0.176	
Y	1.416		1.539		4.345	
REE (ppm)						
La	4.369		1.922		12.52	
Ce	7.522		4.024		22.19	
Pr	0.803		0.483		2.564	
Nd	2.532		1.66		8.566	
Sm	0.379		0.319		1.333	
Eu	0.053		0.064		0.234	
Gd	0.27		0.238		0.977	
Tb	0.043		0.047		0.153	
Dy	0.24		0.26		0.84	
Ho	0.044		0.059		0.162	
Er	0.114		0.157		0.407	
Tm	0.016		0.023		0.065	
Yb	0.1		0.15		0.387	
Lu	0.014		0.02		0.063	
$\sum$REE	16.499		9.426		50.461	
$(La/Yb)_N$	31.34		9.19		23.21	

Note: Major elements for silicates are recalculated after carbonates are extracted from whole-rock.

most of the trace elements are better than 2% (Li et al., 2003). The analytical results are presented in Table 2.

The zircons from two impure marble samples in the Nanshu area are separated for CL imaging and U–Pb dating. The CL imaging was completed at the Institute of Mineral Resource, Chinese Academy of Geological Sciences at Beijing. Zircon U–Pb isotope dating was accomplished by means of SHRIMP II at Beijing whose instrumental conditions and data acquisition were generally described by Compston et al. (1992) and Williams (1998). The U–Pb isotope data were collected in sets of five scans throughout the masses and a reference zircon TEM (417 Ma) was analyzed every fourth analysis. The measured U, Th and Pb abundances as well as Pb isotope ratios were normalized using the reference zircon SL13 (572 Ma) values. Common Pb for the samples was corrected using the measured ^{204}Pb, and errors are reported with 1σ errors; error for the standard calibration was 0.33% (not included in above errors but required when comparing data from different mounts). Common Pb isotope compositions for both the reference TEM and the samples are following the model of Stacey and Kramers (1975) at 417 Ma. All the analyzed results are listed in Table 3. The data were treated following Compston et al. (1992) with the ISOPLOT program of Ludwig (2001), and places on the conventional Wetherwill-type Concordia diagram in $^{206}Pb/^{238}U$ versus $^{207}Pb/^{235}U$ space.

The pure and impure marbles from both the Nanshu and Lugezhung areas were analyzed by the phosphoric acid method for C and O isotopes. CO_2 from calcite was extracted by reaction with phosphoric acid at 25 °C (McCrea, 1950). The selective acid extraction technique proposed by Al-Aasm et al. (1990) was employed when both calcite and dolomite coexisted. C and O isotopic ratios were measured in a Delta+ mass spectrometer at Hefei. The results are reported in the $\delta^{13}C$ notation relative to VPDB and the $\delta^{18}O$ notation relative to VSMOW. The reproducibility of replicate analyses is better than ±0.1‰ for both $\delta^{13}C$ and $\delta^{18}O$ values. Two reference materials of carbonate were used in the isotopic analyses, with $\delta^{13}C = -6.06‰$ and $\delta^{18}O = 5.99‰$ for the National Standard of China GBW04417, and $\delta^{13}C = 1.95‰$ and $\delta^{18}O = 28.59‰$ for the International Standard NBS-19 (Zheng et al., 1998). The results are listed in Table 4.

O isotope analysis of silicate and metal oxide from impure marbles in the Nanshu area was conducted by the laser fluorination technique using a 25W MIR-10 CO_2 laser at Hefei (Zheng et al., 2002). O_2 was directly transferred to the Delta+ mass spectrometer for the measurement of $^{18}O/^{16}O$ and $^{17}O/^{16}O$ ratios. O isotope data are reported as parts per thousand differences (‰) from the reference standard VSMOW in the $\delta^{18}O$ notation. Two reference minerals were used: $\delta^{18}O = 5.8‰$ for UWG-2 garnet (Valley et al., 1995) and $\delta^{18}O = 5.2‰$ for SCO-1 olivine (Eiler et al., 1996). Reproducibility for repeated measurements of each standard on a given day was better than ±0.1‰ (1σ) for $\delta^{18}O$. The results are also listed in Table 4.

4. Results

4.1. Major and trace elements

The major and trace element data for three impure marble samples, 02SD07 and 04SD07 from Nanshu and 02SD16 from Lugezhuang, are presented in

Table 3
SHRIMP Zircon U–Pb isotope data for impure marble 04SD07 at Nanshu in the Jiaobei terrane

Spot	Element contents ($\times10^{-6}$) and ratios					Atomic ratios								Apparent ages (Ma)					
	$^{206}Pb_c$ (%)	U	Th	Th/U	$^{206}Pb^*$	$^{238}U/^{206}Pb^*$	±%	$^{207}Pb^*/^{206}Pb^*$	±%	$^{207}Pb^*/^{235}U$	±%	$^{206}Pb^*/^{238}U$	±%	$^{206}Pb/^{238}U$	1σ	$^{207}Pb/^{206}Pb$	1σ	$^{208}Pb/^{232}Th$	1σ
1.1	0.73	106	53	0.52	26.4	3.46	3.3	0.0983	1.6	3.9143	3.7	0.2888	3.3	1636	48	1591	30	1623	67
2.1	0.10	356	254	0.74	39.3	7.79	3.3	0.06501	1.3	1.1509	3.5	0.1284	3.3	779	24	775	27	830	28
3.1	0.57	269	127	0.49	9.46	24.61	3.4	0.05285	6.8	0.2959	7.6	0.0406	3.4	257	9	322	160	263	17
4.1	0.54	974	520	0.55	114	7.41	3.3	0.06740	1.4	1.2536	3.6	0.1349	3.3	816	25	850	30	807	28
5.1	0.48	320	175	0.56	28.4	9.73	3.3	0.06403	2.2	0.9076	3.9	0.1028	3.3	631	20	743	47	739	27
6.1	5.98	83	68	0.85	10.3	7.33	3.5	0.0887	11	1.6682	11	0.1364	3.5	824	27	1399	200	989	86
7.1	0.50	146	43	0.31	15.6	8.08	3.4	0.0628	3.7	1.0711	5.0	0.1237	3.4	752	24	703	78	759	52
8.1	1.04	408	111	0.28	44.1	8.04	3.3	0.0679	3.8	1.1646	5.0	0.1244	3.3	756	24	865	78	762	60
9.1	0.35	1652	318	0.20	85.2	16.72	3.3	0.05949	1.3	0.4905	3.5	0.0598	3.3	374	12	585	28	533	21
10.1	1.22	91	43	0.48	9.63	8.26	3.4	0.06587	5.3	1.0998	6.3	0.1211	3.4	737	24	803	120	706	46

Note: Pb_c, common Pb; Pb*, radiogenic Pb; Using measured ^{204}Pb for common Pb correction. Uncertainties on the atomic ratios are at 1σ.

Table 4
Oxygen and Carbon isotope compositions of mineral separates from marbles from the Jiaobei terrane in the Sulu orogen

Sample number	Host rock	Locality	Mineral	$\delta^{18}O$ (‰) (VSMOW)	$\delta^{13}C$(‰) (VPDB)	Mineral pair	O isotope temperature (°C)
02SD06	Marble	Nanshu	Dolomite	14.31	1.00		
			Calcite	12.86	3.93	Dol–Cc	Equilibrium
02SD07	Impure marble	Nanshu	Dolomite	20.20	2.30	Dol–Cc	Equilibrium
			Calcite	18.92	1.76	Cc–Gt	680
			Garnet	15.82			
02SD08	Marble	Nanshu	Calcite	13.13	−0.93		
04SD07	Impure marble	Nanshu	Calcite	19.32	1.08	Cc–Mus	165
			Muscovite	14.27			
04SD08	Olivine aggregate	Nanshu	Magnetite	7.45			
04SD11	Impure marble	Nanshu	Calcite	17.24	−0.23	Cc–Mus	280
			Muscivite	13.37			
02SD16	Impure marble	Lugezhuang	Dolomite	18.60	4.18		
			Calcite	20.03	3.60	Dol–Cc	Disequilibrium
02SD17	Marble	Lugezhuang	Dolomite	23.44	5.56		
			Calcite	23.82	5.06	Dol–Cc	Disequilibrium

Abbreviations: Cc, calcite; Dol, dolomite; Gt, garnet; Mus, muscovite. *Note*: Calculation of calcite–garnet or calcite–muscovite O isotope temperatures is based on the calibration of Zheng (1993a,b); Equilibrium or disequilibrium judgement of dolomite–calcite O isotope fractionation is based on the calibration of Zheng (1999).

Table 2. They are high in SiO_2 (13.10–17.63%), MgO (21.46–23.21%) and CaO (29.06–30.77%), but low in Al_2O_3 (0.71–1.58%), Fe_2O_3 (0.01–0.62%), Na_2O (0.00–0.03%), K_2O (0.00–0.25%), TiO_2 (0.01–0.03%) and P_2O_5 (0.01–0.02%). The calculated composition of major elements for the impure materials (Table 2) within the marbles suggests that they may be highly magnesian and moderately siliceous. Because of high mobility for some elements during metamorphism and hydrothermal alteration, the observed composition of major elements may not truly represent their protolith limestone or impure limestone. For example, the contents of FeO for the impure marbles are extremely low, which can be ascribed to significant Fe^{2+} loss during intensive serpentinization for olivine (Bucher and Frey, 2002).

With respected to the composition of REE and trace elements, the impure marbles generally have similar REE partition patterns showing variable LREE enrichment with $(La/Yb)_N$ of 9.19–31.34, weakly Eu negative anomaly and significant HREE depletion with gentle slope (Fig. 3). This is somewhat similar to commonly observed patterns for sedimentary carbonates (e.g., Boulvais et al., 2000). On the primitive-mantle-normalized spider diagram, the trace elements display similar LILE-rich patterns with variable abundances, significant positive anomalies in Th, U and Sr but pronounced negative anomalies in Nb, Ta and Ti (Fig. 4).

In general, samples 02SD07, 02SD16 and 04SD07 are similar in the composition of major and trace elements, suggesting similar protoliths for the impure marbles at Nanshu and Lugezhuang. Furthermore, 04SD07 that has more silicate contents (Table 1) is relatively higher in REE and trace elements (Table 2), indicating that the observed REE and trace element patterns (Figs. 3 and 4, respectively) are principally controlled by the presence of silicate minerals within the impure marbles. How-

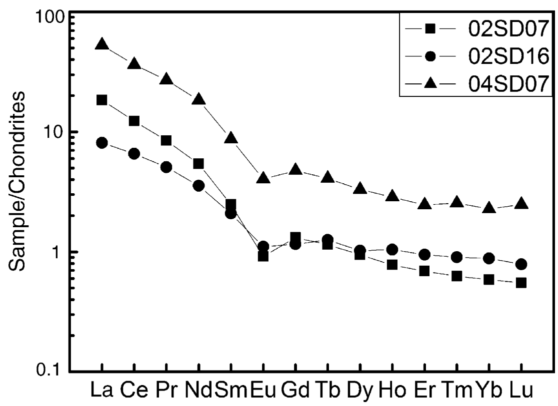

Fig. 3. Diagram of chondrite-normalized REE for impure marbles from the Jiaobei terrane in the Sulu orogen. Chondrite values are after Sun and McDonough (1989).

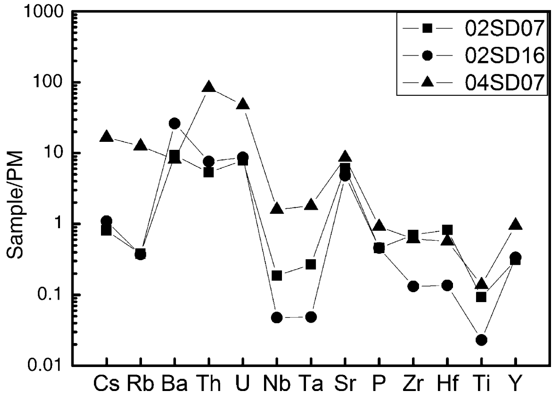

Fig. 4. Diagram of primitive mantle-normalized trace elements for impure marbles from the Jiaobei terrane in the Sulu orogen. Primitive mantle values are after Sun and McDonough (1989).

ever, the positive Sr anomaly may be caused by mixing between the silicate and carbonate minerals, and the variable LILE abundances may be the result of metamorphic disturbance.

4.2. Zircon U–Pb dating

Zircons from sample 02SD07 are generally colorless, transparent, and anhedral to subhedral. Crystal lengths range from ca. 80 to 150 μm, with ratios of length/width ranging from 1:1 to 2:1. CL imaging reveals that most grains have clear core-rim structure (Fig. 5a). The cores show oscillatory zoning, weakly zoning or patched zoning, which are magmatic but have differently been modified by metamorphism. The rims exhibit no zoning or cloudy zoning, and some have irregular boundaries truncating the primary oscillatory zoning cores, which are typical for metamorphic zircons. A few grains wholly show similar internal structures as the rims, indicating their metamorphic genesis.

A total of eight U–Pb isotope analyses were made on seven zircons from sample 02SD07 (Fig. 6a), three of which were on igneous zircons that clearly show the magmatic zoning, and five of which were on metamorphic zircons that either suffered intensive recrystallization or are new growth. The three igneous zircon spots give the $^{207}Pb/^{206}Pb$ ages of 682 ± 160 to 763 ± 180 Ma with Th/U ratios of 0.62–0.90, the five metamorphic zircon spots give the $^{206}Pb/^{238}U$ ages of 218 ± 5 to 312 ± 6 Ma with Th/U ratios of 0.17–0.80 (Tang et al., 2004). As shown in Fig. 6a, all eight spots define a discordia chord which intercepts the concordia curve at 769 ± 48 and 215 ± 48 Ma (MSWD = 0.081), respectively, corresponding to the Neoproterozoic crystallization and the Triassic metamorphism.

Zircons recovered from sample 04SD07 are light yellow, transparent and subhedral. The lengths of these grains scatter between 80 and 200 μm, with length/width ratios of 1.5:1 to 2:1. In CL images, most grains preserve oscillatory zoning, which is disrupted by patched or weakly zoning domains with stronger brightness that cut oscillatory zoning (Fig. 5b). Resorption structures are preserved around some grains. These results suggest that they are magmatic zircon and suffered different degrees of metamorphic recrystallization in the presence of fluid. Thin and not zoned rims occasionally occur around some grains with dark CL, which are interpreted as metamorphic domains. A few broken grains show no zoning, which may be inherited detrital zircons that suffered metamorphic recrystallization.

A total of 10 U–Pb isotope analyses were made on 10 zircons from sample 04SD07 (Fig. 6b), eight of which were on igneous zircons with magmatic zoning, and two of which were on metamorphic zircons with significant recrystallzation. As listed in Table 3, six igneous zircon spots give the $^{207}Pb/^{206}Pb$ ages of 703 ± 78 to 865 ± 78 Ma with Th/U ratios of 0.28–0.79, and two igneous zircon spots give $^{207}Pb/^{206}Pb$ ages of 1399 ± 200 to 1591 ± 30 Ma with Th/U ratios of 0.52–0.85, and two metamorphic zircon spots give the $^{206}Pb/^{238}U$ ages of 257 ± 9 to 374 ± 12 Ma with Th/U ratios of 0.20–0.49. These 10 analysis spots define two discordia chords in Fig. 6b. The discordia chord that has eight spots gives intercept ages of 813 ± 37 and 238 ± 75 Ma (MSWD = 3.4), respectively. The upper intercept age of 813 ± 37 Ma is consistent with the weighted mean $^{207}Pb/^{206}Pb$ age of 767 ± 38 Ma (MSWD = 1.6) of the five concordant spots within analytical error, suggesting the Neoproterozoic crystallization for the igneous zircons. Meanwhile, the lower intercept age of 238 ± 75 Ma is responsible for the Triassic metamorphism. The discordia chord which has only three spots gives intercept ages of 1587 ± 32 and 249 ± 20 Ma (MSWD = 0.076), respectively (Fig. 6b). The upper intercept age of 1587 ± 32 Ma is consistent with a concordant $^{207}Pb/^{206}Pb$ spot-age of 1591 ± 30 Ma (spot 1.1 in Table 3) within analytical errors and is the best estimate for the crystallization of Paleoproterozoic igneous zircon. Low U contents of 83–106 ppm are also associated with the two oldest zircons (Table 3), suggesting a different population from the other zircons. The lower intercept age of 249 ± 20 Ma, consistent with the former lower intercept age within analytical errors, is also correspond to the same Triassic metamorphic overprint.

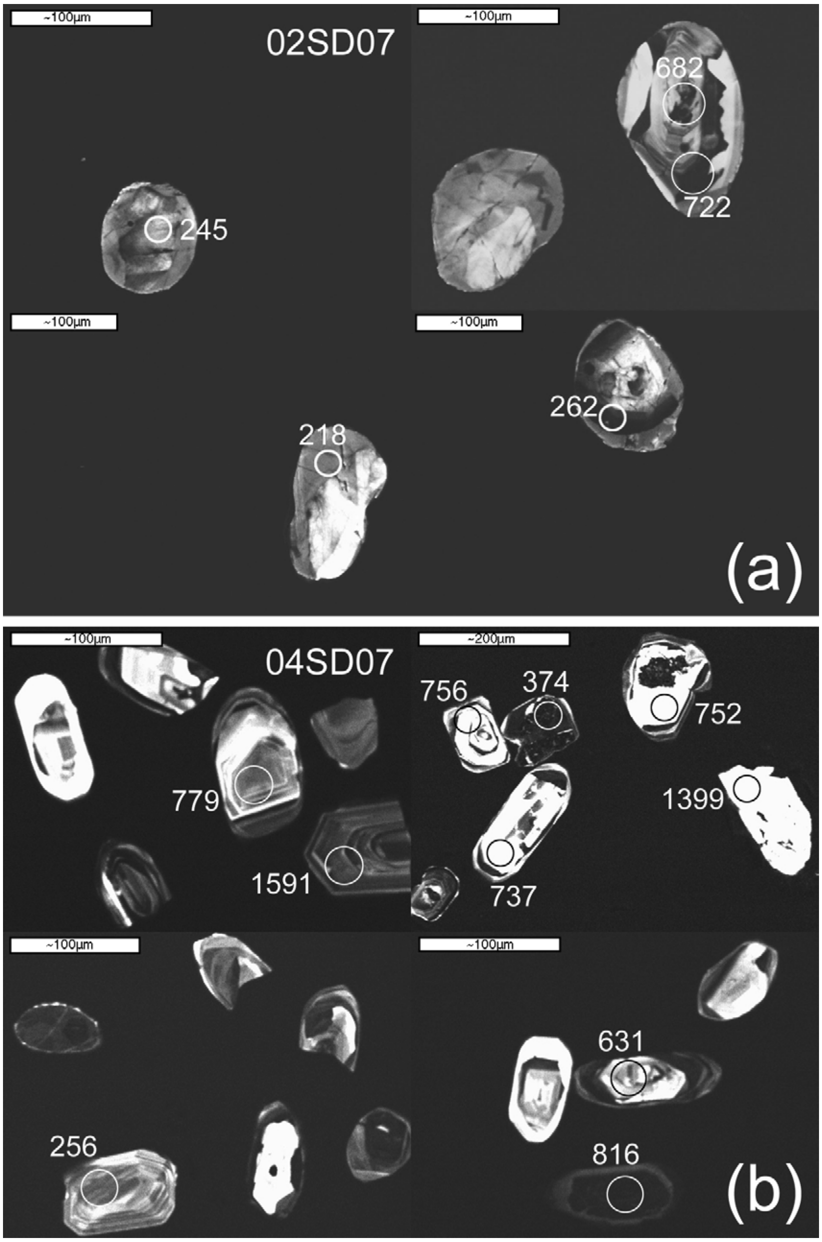

Fig. 5. CL images and U–Pb ages for zircons from impure marble at Nanshu in the Jiaobei terrane.

4.3. Marble C and O isotopes

The C and O isotope compositions of carbonate minerals (calcite and dolomite) from the marbles at Nanshu and Lugezhuang show wide variations (Table 4). The values of $\delta^{13}C$ (relative to VPDB) are −0.9 to 5.1‰ for calcite and 1.0–5.6‰ for dolomite; the values of $\delta^{18}O$ (relative to VSMOW) are 12.9–23.8‰ for calcite and 14.3–23.4‰ for dolomite. Relatively, the marbles at Lugezhuang have higher values of $\delta^{13}C$ and $\delta^{18}O$ than those at Nanshu. The samples contain insufficient fresh olivine to allow for O isotope analysis. However, the other silicate separates from the impure marbles have high $\delta^{18}O$ values, 13.4–14.3‰ for muscovite and 15.8‰ for garnet, respectively (Table 4).

In general, there is a positively correlated trend between $\delta^{13}C$ and $\delta^{18}O$ values for the marbles in question (Fig. 7a), indicating variable magnitudes of rock–fluid interaction at high temperature for the marble protolith (limestone) at Nanshu. The metamorphic

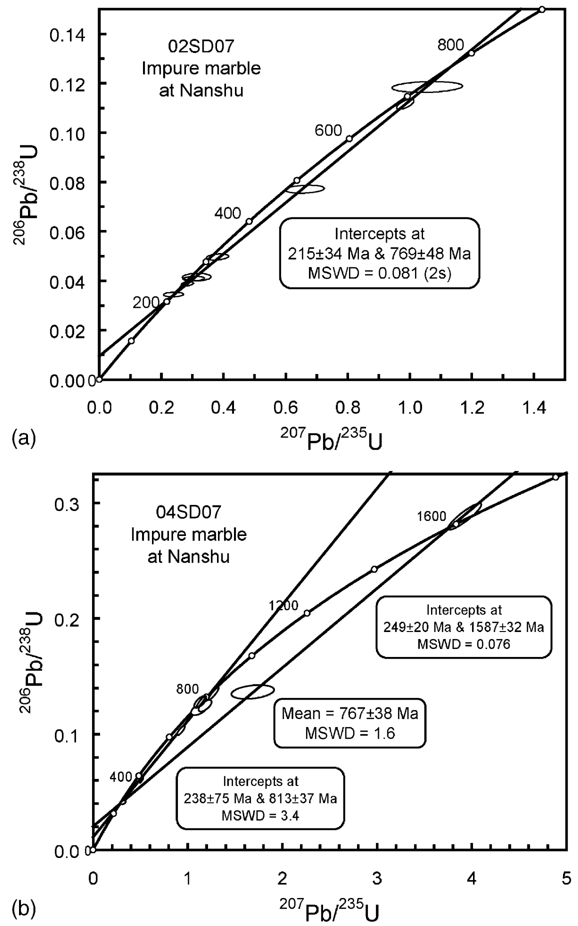

Fig. 6. U–Pb Concordia diagram for zircons from impure marble at Nanshu in the Jiaobei terrane. Data source: 04SD07 (this study) and 02SD07 (Tang et al., 2004).

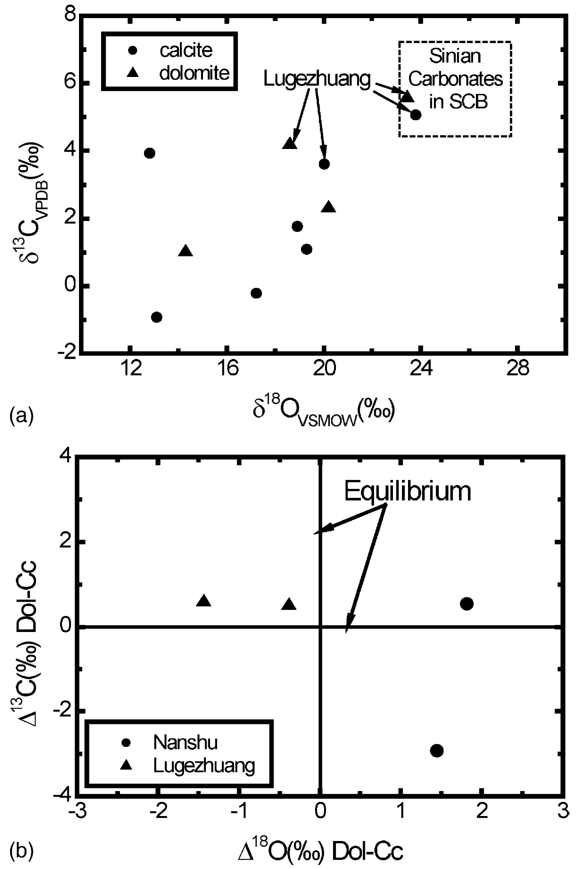

Fig. 7. (a) Carbon and oxygen isotope diagram for marbles from the Jiaobei terrane in the Sulu orogen. (b) $\Delta^{18}O$–$\Delta^{13}C$ diagram for marble at Nanshu and Lugezhuang in the Jiaobei terrane.

garnet from sample 02SD07 has the high $\delta^{18}O$ value of 15.8‰, and is in O isotope equilibrium with calcite at the high-grade metamorphic conditions (680 °C in Table 4), suggesting that the high temperature rock–fluid interaction took place prior to the high-grade metamorphism. However, the highest values of $\delta^{13}C$ and $\delta^{18}O$ for the marbles at Nanshu, 3.93 and 20.20‰, respectively, are close to those of marbles at Lugezhuang, suggesting that the marble protoliths in these two areas probably have the similar C and O isotope compositions.

5. Discussion

5.1. *U–Pb radiometric system of carbonate and zircon*

Application of carbonate Pb–Pb and U–Pb dating has contributed a lot to timing of limestone deposition or marble metamorphism (Moorbath et al., 1987; Jahn, 1988; Jahn et al., 1990; Taylor and Kalsbeek, 1990; Jahn and Cuvellier, 1994; Woodhead and Hergt, 1997; Wang et al., 1998; Fölling et al., 2000). However, difficulties were encountered in obtaining reasonable isochrons because the U–Pb isotopic system of carbonate rocks is prone to disturb by diagenesis or retrograde alteration. As illustrated in this study, zircon SIMS U–Pb dating coupled with CL imaging can be a successful way to constrain the impure marble on its ages of both protolith deposition and metamorphism.

As shown in Table 3, the Triassic metamorphic zircons from our samples of impure marble generally have relatively lower Th/U ratios relative to the Neoproterozoic igneous zircons, but Th/U ratios in most of the metamorphic zircons are >0.2. It is known that metamorphic zircon generally has Th/U ratio of less than 0.1–0.2 (e.g., Rubatto et al., 1999; Hoskin and Schaltegger, 2003), but the Th/U ratios up to 0.70 were also observed in some metamorphic zircons (e.g., Vavra et al., 1999). Therefore, the Th/U ratio alone cannot be a valid reference to distinguish the metamorphic zircon from igneous zircon in this study.

On the other hand, the morphology, CL imaging and U–Pb age for our samples (Fig. 5 and Table 3) suggest that most of the zircons in question are the Neoproterozoic igneous zircons which have magmatic zoning with relatively higher Th/U ratios, but some of the igneous zircons that have unzone or patchy zone CL patterns with relatively lower Th/U ratios indicate recrystallization during the Triassic metamorphism. A few metamorphic zircons have the concordant Triassic ages with the unzoning CL patterns (such as 02SD07 spot 7.1 in Table 3), suggesting either complete recrystalization or new growth during the Triassic metamorphism. The upper intercept age of 769 ± 48 Ma from 02SD07 is consistent with the concordia age of 767 ± 38 Ma and the upper intercept age of 813 ± 37 Ma from sample 04SD07 within the analytical error, and is regarded as the crystallization age of the Neoproterozoic igneous zircons. The lower intercept age of 215 ± 48 Ma from 02SD07 is also consistent with the two lower intercept ages of 238 ± 75 and 249 ± 20 Ma from sample 04SD07 within analytical error, and is regarded as the Triassic metamorphism age. Meanwhile, the two Paleoproterozoic igneous zircons found in sample 04SD07 also experienced the Triassic metamorphism.

5.2. Marble C and O isotope systems

The normal marine limestone has the $\delta^{13}C$ values of 0 ± 2‰ and $\delta^{18}O$ values of >+28‰ (Hoefs, 2004), the metamorphic devolatilization can only result in decrease of a few per mil in both $\delta^{13}C$ and $\delta^{18}O$ in the absence of external fluid infiltration (Valley, 1986; Hoefs, 2004). However, the interaction with H_2O-dominant fluid at high temperature can dramatically change both $\delta^{13}C$ and $\delta^{18}O$ values for the limestone (e.g., Guerrera et al., 1997; Zheng et al., 1998). Because there is no geochemical process to enrich carbonate in ^{13}C during regional metamorphism (e.g., Valley, 1986; Hoefs, 2004), the observation that more than a half of our marble samples have $\delta^{13}C$ values >2‰ (Table 4) undoubtedly reflect a positive C isotope anomaly for the marble protolith (limestone).

Theoretically, the values of equilibrium fractionation for $\delta^{13}C$ and $\delta^{18}O$ between dolomite and calcite are both ≥0‰ (Zheng, 1999). Except for sample 02SD06 from Nanshu that shows a negative dolomite–calcite fractionation of −2.93‰ (Table 4) and thus suggests C isotope disequilibrium, the rest three samples of marble have positive dolomite–calcite fractionations of 0.50–0.58‰ and thus are at C isotopic equilibrium with each other (Fig. 7b). The equilibrium C isotope fractionations between dolomite and calcite indicate that the C isotope system of marbles was not disturbed by the later metamorphism and thus the positive $\delta^{13}C$ values for the marbles are inherited from their precursor limestone. In contrast, the disequilibrium C but equilibrium O isotope fractionations between dolomite and calcite in sample 02SD06 may suggest that rates of carbonate precipitation have kinetic effects on C isotope fractionation between precipitated $CaCO_3$ and dissolved HCO_3^- (Turner, 1982; Romanek et al., 1992).

The marbles at Nanshu are at O isotopic equilibrium, but those at Lugezhuang are obviously at O isotopic disequilibrium (Fig. 7b). The O isotopic disequilibrium relationship between dolomite and calcite can be ascribed to one of the following three processes: (1) interaction between marble and low-$\delta^{18}O$ fluid at relatively lower temperatures (<300 °C) at shallow levels during retrograde metamorphism. In this case, the rate of O diffusion in calcite is faster than that in dolomite (O'Neil, 1987), causing greater depletion of ^{18}O in calcite than that in dolomite; (2) polymorphic transformation of aragonite into calcite during diagenesis. The component of $CaCO_3$ can deposit as aragonite in sedimentary environment, the $\delta^{18}O$ value of aragonite is 1–3‰ lower than that of calcite when aragonite is in O isotope equilibrium with coexisting calcite at anhydrous medium (Zheng, 1999). However, the aragonite is unstable and will transform quickly into calcite (Zhou and Zheng, 2001, 2002, 2003, 2005), and the calcite can inherit the O isotope composition from aragonite during the polymorphic transformation without dissolution–reprecipitation (Zheng, 1999; Zhou and Zheng, 2005); (3) hydrothermal alteration for calcite by an ^{18}O-rich fluid during diagenesis and metamorphism. As a result, the $\delta^{18}O$ value for calcite became greater than that for coexisting dolomite.

The occurrences of the secondary muscovite (Fig. 2f) and olivine serpentinization (Fig. 2a) in the impure marbles in the Nanshu and Lugezhuang areas undoubtedly indicate fluid activity during retrograde metamorphism, and both ^{18}O-depleted and enriched fluids were involved. Therefore, the rock–fluid interaction during retrograde metamorphism is likely responsible for the O isotopic disequilibrium between dolomite and calcite for the marbles at Lugezhuang. However, the preservations of C isotopic equilibrium between calcite and dolomite as well as the high $\delta^{18}O$ values for muscovite imply that the rock–fluid interaction has an insignificant influence on the values of both $\delta^{13}C$ and $\delta^{18}O$ for the marbles during the retrograde metamorphism. This implies that the C content in the retrograde fluid is very limited or the C and O isotopic compositions of the fluid are similar to those of the marbles.

5.3. Marble metamorphism

It is generally known that the olivine-rich marble is the metamorphic product, usually occurred within either contact zones between marbles and intrusions or high-grade regional metamorphic massifs (Holness et al., 1991; Bucher and Frey, 2002). There are no intrusion outcropped near the impure marbles at Nanshu and Lugezhuang, the possibility of contact metamorphism is precluded. Previous petrologic investigations suggest that the Fenzishan Group underwent the upper amphibolite-facies to granulite-facies metamorphism (Wang, 1995; Zhai et al., 2000; Zhou et al., 2001, 2004a,b), therefore, the impure (olivine-rich) marbles in question are likely related to high-grade metamorphism. The O isotope temperature of 680 °C for the calcite-garnet pair from sample 02SD07 (Table 4) just indicates the metamorphic conditions of upper amphibolite-facies for the impure marble.

The zircon SHRIMP U–Pb dating for the impure marble gave the discordia lower-intercept ages of 215 ± 48, 238 ± 75 and 249 ± 20 Ma (Fig. 6). Because of the occurrence of sector or no zoning in the dated zircons (Fig. 5), a weighted mean age of 240 ± 44 Ma is obtained with MSWD = 1.5 (Fig. 8a), clearly reflecting the Triassic metamorphism for the impure marble. This age is consistent with the UHP metamorphic ages in the Dabie-Sulu orogenic belt (e.g., Ames et al., 1996; Li et al., 1999; Zheng et al., 2003, 2004), and provide the geochronological evidence for the influence of SCB–NCB collision on the Jiaobei terrane.

Theoretically, the components of SiO_2 and Al_3O_2 in metamorphic reaction with dolomite for garnet, clinopyroxene or olivine, can come from either sialic material in impure marbles or external H_2O-dominant fluids that immigrate along the faults or contact boundaries (Bucher and Frey, 2002). The depths of the high-grade metamorphism (upper amphibolite-facies to granulite-facies) for the Fenzishan Group were more than 30 km (Wang and Lin, 1991; Zhou et al., 2001), at which no external H_2O-dominant surface fluids can reach. The garnet and muscovite in question both have the high $\delta^{18}O$ values and are in O isotope equilibrium with calcite (Table 4). These observations indicate that the components of SiO_2 and Al_3O_2 in the marbles were likely derived from the impure marbles itself rather than external H_2O-dominant surface fluids which typically have lower $\delta^{18}O$ values of ∼0‰. Therefore, the sialic material in the marbles was either terrigenous deposits or subwater volcaniclastic rocks that were deposited synchronously with the limestone. The banded segregates of olivine in marbles imply that the sialic material originally occurred as thin layers within marbles. In the light of zircon morphology and zircon internal structure as well as zircon U–Pb ages (see detailed discussion in Section 5.2), we suggest that the thin layers of sialic material were probably the subwater volcaniclastic rocks that were deposited synchronously with the limestone (see arguments below).

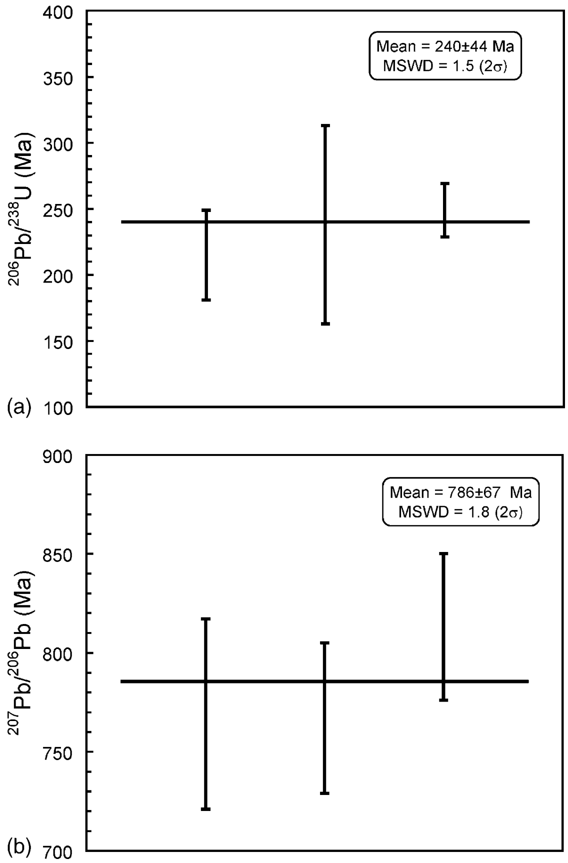

Fig. 8. Weighted mean age of metamorphic (a) and igneous (b) zircons from impure marble at Nanshu in the Jiaobei terrane.

5.4. Nature of marble protolith

The igneous zircons of mid-Neoproterozoic age in the impure marbles could be derived from either terrigenous detritus or volcaniclastic rocks that were deposited synchronously with the limestone, marble protolith. The other silicate minerals also occur in the impure marble, but they are of metamorphic genesis (Fig. 2). We propose that the zircons and other silicates were derived from the volcaniclastic deposits according to the following observations: (1) most of the zircons are of igneous origin with clearly prismatic and pyramid faces (Fig. 5), indicating that the zircons did not experience abrasion by long-distance mechanical transportation. Although some of the zircons have rounded shape, the CL images and the U–Pb ages demonstrate that these grains were principally of fluid infiltrated during Triassic metamorphism rather than abrasion origin; (2) the long-distance transportation would cause the detrital zircons of terrigenous origin in marine strata to not only have complicated U–Pb age-pattern responsible for multi-terrigenous provenances, but also have pitted surface and micro-fracture by mechanical abrasion (Fedo et al., 2003). The igneous zircons in our samples mostly gave the consistent mid-Neoproterozoic ages (except for two grains), suggesting that the zircons were predominantly derived from a single igneous source; (3) the occurrence of banded olivine segregates (Fig. 2b) indicates that the silicate material originally occurred as thin layers within the limestone, probably corresponding to volcaniclastic layers; (4) the sedimentary facies analyses for the Fenzishan Group suggested several times of marine volcanic activity during the sedimentation of the Fenzishan limestone in the rift basin (Lin et al., 1998). Therefore, the mid-Neoproterozoic zircons in the impure marble were derived from the product of rift volcanism that has been demonstrated for the UHP metaigneous rocks in the Dabie-Sulu orogenic belt (Zheng et al., 2003, 2004).

The zircons that show the oscillatory zoning typical of igneous origin (Fig. 5) yielded the U–Pb discordia upper-intercept ages of 769 ± 48 and 813 ± 37 Ma as well as the weighted mean age of 767 ± 38 Ma (Fig. 6). A weighted mean of these three ages yields an age of 786 ± 67 Ma with MSWD = 1.8 for the impure marble (Fig. 8b), which is in agreement with the protolith ages of 700–800 Ma for the UHP metaigneous rocks in the Dabie-Sulu orogenic belt (e.g., Ames et al., 1996; Hacker et al., 1998; Zheng et al., 2003, 2004). It appears that the mid-Neoproterozoic ages represent the timing of zircon crystallization from the magmas that were emplaced along the northern edge of the South China Block in response to the breakup of Rodinia supercontinent. The two zircon grains with the discordia intercept ages of 1587 ± 32 and 249 ± 20 Ma (Fig. 6b) are also consistent with the known dates for a few eclogite and paragneiss in the Dabie-Sulu orogenic belt (e.g., Ames et al., 1996; Zheng et al., 2003; Li et al., 2004), suggesting the presence of few older detritus in the impure marble with the same influence by the Triassic metamorphism.

The C isotope composition of marbles can be used to trace the sedimentary environment of their protolith (e.g., Wickham and Peters, 1993; Boulvais et al., 1998; Zheng et al., 1998; Rumble et al., 2000; Melezhik et al., 2005). In particular, the positive δ^{13}C anomaly in Neoproterozoic limestones (900–570 Ma) has been found to be global events, which are presumably related to the Sturtian glaciation (750–710 Ma) and the Marinoan glaciation (660–635 Ma) in the snowball Earth hypothesis (Hoffman et al., 1998; Hoffman and Schrag, 2002; Kennedy et al., 1998; Prave, 1999; Fanning and Link, 2004; Hoffmann et al., 2004). There are two equivalent glacial horizons, called the Gucheng (or Chang'an) and the Nantuo tillites, respectively, occurring on the South China Block (Ma et al., 1984; Zhang and Piper, 1997; Evans et al., 2000; Yin et al., 2003; Wang and Li, 2003; Zhou et al., 2004a; Chu et al., 2005; Condon et al., 2005; Zhang et al., 2005). The predominantly positive δ^{13}C values of −0.9 to 5.6‰ are also obtained for the marbles from the Jiaobei terrane (Fig. 7a). This is not only consistent with positive δ^{13}C values for the Doushantuo and Dingying Formations of Sinian limestones on the South China Block (Lambert et al., 1987; Shen, 2002), but also in agreement with positive δ^{13}C values for the UHP metamorphosed marbles in the Dabie orogen (Zheng et al., 1998; Rumble et al., 2000).

In view of the U–Pb ages of 786 ± 67 Ma for the volcanogenic zircons from the impure marbles (Fig. 8b), therefore, the sedimentary timing of Fenzishan limestone (marble protolith) can reasonably be constrained to occur during the middle Neoproterozoic, a possible period of 761 ± 8 to 663 ± 4 Ma for the Sturtian glaciation in South China (Zhou et al., 2004a). The high δ^{18}O values of 13.4–15.8‰ for the garnet and muscovite from the impure marble indicate that the silicates were deposited chemically rather than detritally together with the limestone. If protolith of the impure marble is assumed to be a kind of impure limestone, the occurrence of mid-Neoproterozoic zircons together with the other silicates indicate an incorporation of volcaniclastic rocks during the limestone deposition at the mid-Neoproterozoic. This indicates that the sedimentary environment of the Fenzishan Group is more close to the South China Block rather than the North China Block.

6. Implication for tectonic affinity

The Jiaobei terrane is a critical region to locate the Triassic suture boundary between the South China Block and the North China Block. Geotectonically, the Jiaobei terrane is ascribed to the southern edge of NCB (Cong and Wang, 1999; Wallis et al., 1999; Zhai et al., 2000; Zhao et al., 2001), and thus the NCB–SCB suture zone is generally considered along the Wulian-Yantai fault (Cong and Wang, 1999; Zhai et al., 2000), responsible for the northern margin of the Sulu UHP metamorphic belt (Fig. 1b). On the basis of structure analysis and petrological study, however, Faure et al. (2001) argued that the suture should lie north of the Penglai Group rather than the Wulian-Yantai fault (Fig. 1). Because of its importance in studying the geodynamic evolution of a collisional orogenic belt, debate on the suture location in the Sulu orogen has attracted much attention (e.g., Cong and Wang, 1999; Faure et al., 2001, 2002, 2003; Zhai et al., 2000; Zhai, 2002; Wu et al., 2004; Zheng et al., 2005).

The Fenzishan Group uncomformably underlies the Penlai Group, both of them being equally important with respect to their tectonic affinity between SCB and NCB. Due to lacking of precisely geochronological data, however, the protolith and metamorphism ages of the Fenzishan Group were poorly understood (Wang, 1995; Zhao et al., 1995). The occurrence of Neoproterozoic igneous rocks is a critical reference for discriminating SCB from NCB (Hacker et al., 1998; Wan and Zeng, 2002; Wu et al., 2004), especially for the petrotectonic units close to the NCB–SCB suture zone (Zheng et al., 2005). On the basis of our combined study of zircon U–Pb dating, C–O isotopes and petrography of impure marble, the occurrence of mid-Neoproterozoic carbonates with the Triassic metamorphism and the positive C isotope anomaly is identified in the Fenzishan Group. This demonstrates that both mid-Neoproterozoic magmatism and Triassic metamorphism are recorded in the studied targets. Therefore, the Fenzishan marbles geotectonically belong to SCB, and its protolith corresponds to the sedimentary limestone that was deposited in the rift basin during the mid-Neoproterozoic along the northern margin of SCB.

It is usually assumed that the Wulian-Yantai fault marks the SCB northern margin in the Sulu orogen and the Jiaobei terrane geotectonically belongs to the NCB southern edge of NCB. The occurrence of the Fenzishan marbles with the SCB affinity, however, seems to challenge this assumption. In other words, the Jiaobei terrane could be interpreted as the SCB northern edge rather than the NCB southern edge. If the Fenzishan marbles and their underlying basement would bond together since the Neoproterozoic, the Jiaobei terrane would geotectonically correspond to the northern edge of SCB. In this regard, the Wulian-Yantai fault would not be the NCB–SCB suture boundary in the Sulu orogen. According to the similarity of petrologic and structural features in the north zone between the Dabie and Sulu regions and the lack of oceanic basin lithologies in the Sulu region, Faure et al. (2001, 2002) postulated that the NCB–SCB suture boundary lies north of the Penglai Group in the northeastern part of the Sulu region (Fig. 1). However, this postulation is in conflict with the common consensus that the Wulian-Weihai fault marks the northern margin of the UHP metamorphic zone and thus represents the collision suture between the two plates east of the Tanlu fault (e.g., Wang and Cong, 1998; Cong and Wang, 1999; Zhai et al., 2000; Zhai, 2002; Yang, 2002).

Instead, the occurrence of the Fenzishan marbles with both mid-Neoproterozoic igneous and Triassic metamorphic zircons on the Jiaobei terrane does not mean that the Jiaobei terrane belongs to SCB. A tectonic decoupling is suggested to occur between the Fenzishan marbles and the underlying basement during the Triassic continent–continent collision. Therefore, we present a crustal detachment model to explain the unusual occurrence by northward thrust of the SCB marbles over the NCB basement. It is inferred that during the Triassic continent subduction, the cover limestone in the northern margin of SCB was not only detached from the SCB basement, but also northward thrusted for tens of kilometers over the NCB southern margin (Fig. 9a). At the same time, it experienced the amphibolite-facies metamorphism to result in the formation of impure marbles. Emplacement of Early Cretaceous igneous rocks brought about the outcrop of the different grades of metamorphic rocks in the Sulu orogen and its adjacent NCB southern margin. As a result, the Fenzishan marbles in SCB affinity occurs above the NCB southern margin and thus north of the Wulian-Yantai fault (Fig. 9b).

The crustal detachment, essentially similar to flake tectonics or tectonic wedging, is a common feature during continental collisions (e.g., Oxburgh, 1972; Price, 1986; Ellis, 1988; Stockmal et al., 1990; Li, 1994; Lin et al., 1994; Zheng et al., 2005). Because sedimentary cover of the upper crust is relatively buoyant and thus resists continuing subduction of continental lithosphere, it is split from the underlying basement to form a thin-flake. It can not only thrust above the overriding plate as observed in this study, but also accumulate as a deformed passive-margin accretionary wedge along the suture zone between two collided continents (Zheng et al., 2005). A crustal detachment model was also proposed by Li (1994) to explain the decoupling that the surface suture occurs in the Sulu orogen but a deep suture lies much southwards in Nanjing, parallel to the Lower Yangtze Valley fault zone. Nevertheless, the high O isotope temperature of 680 °C from the calcite–garnet pair in the impure marble at Nanshu implies that the detached cover may experience shallow subduction up to the upper amphibolite-facies conditions. Because of its buoyancy relative to the basement, the subducted cover would be detached from the basement for exhumation

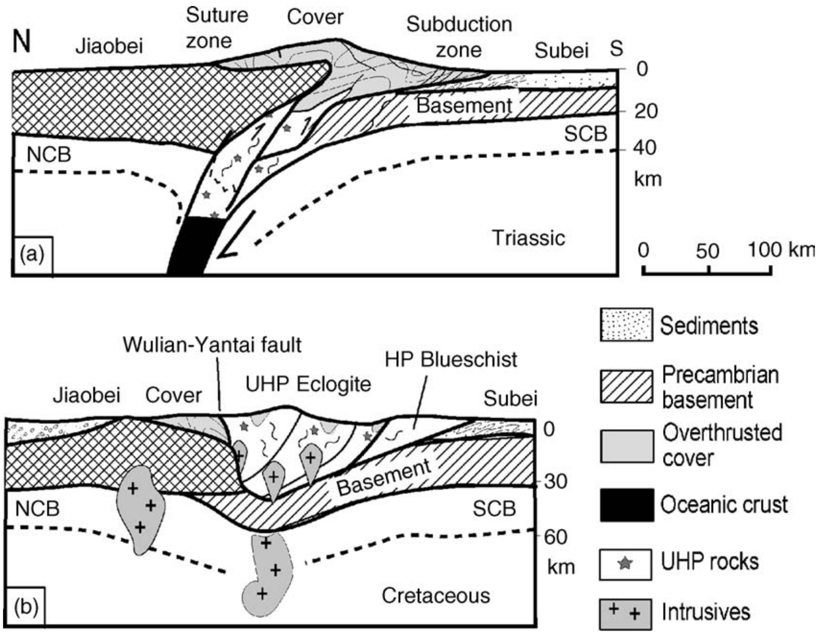

Fig. 9. A crustal detachment model to explain the occurrence of the Fenzishan marbles with geotectonic affinity to the South China Block overlying the southern margin of the North China Block in the Sulu orogen. (a) Triassic subduction of SCB beneath NCB brought about a crustal detachment of sedimentary cover from crystalline basement to result in northward thrusting over the NCB southern margin, whereas the SCB basement and underlying mantle lithosphere were further subducted to mantle depths along the suture marked by the Wulian-Yantai fault. Deformation-metamorphism is expected to occur not only in the overthrusted cover (a part of passive-margin accretionary wedge as defined by Zheng et al., 2005), but also in its front responsible for the NCB southern margin. (b) Emplacement of Early Cretaceous igneous rocks caused outcrop of metamorphic rocks in the Sulu orogen and the NCB southern margin, resulting in the present observation that the Fenzishan marbles with the SCB affinity unusually occur above the NCB basement in the Jiaobei region.

along subduction channel. It was then thrusted over the southern margin of the North China Block due to the continuing subduction of the South China Block.

The tectonic overthrust by the crustal detachment between cover and basement can well explain the unusual occurrence of the Fenzishan marbles in the SCB affinity above the NCB southern margin in the Jiaobei terrane. This sheds light on the previous debates concerning the suture location between SCB and NCB in the east-central China (e.g., Cong and Wang, 1999; Faure et al., 2001, 2002, 2003; Zhai et al., 2000; Zhai, 2002; Wu et al., 2004; Zheng et al., 2005). The occurrence of mid-Neoproterozoic magmatic products in this region does not negate the contention that the suture location lies along the Wulian-Yantai fault that marks the northern margin of the UHP metamorphic belt. More important is that both metamorphism and deformation are associated with the overthrusting process. This may be the reason why the similar features of structural deformation to those in the northern part of the Dabie orogen were observed by Faure et al. (2001, 2002, 2003) in the Wulian–Penglai Groups low-grade metamorphic rocks and some basement rocks in the northern part of the Sulu orogen (i.e., the Jiaobei terrane, the northern part of the Shandong Pennisula). A large-scale overthrust over 200 to 300 km distance could be brought about by the crustal detachment during the Triassic subduction of the South China Block beneath the North China Block. This may provide a resolution to the controversy concerning the decoupling in the suture boundary between surface and depth in the northern part of the Shangdong Peninsula.

7. Conclusions

A successful zircon SHRIMP U–Pb dating for the impure marbles from the Fenzishan Group in the Jiaobei terrane demonstrates that it is a powerful means to date the deposition and metamorphism for impure carbonates if the zircons deposit synchronously with them. Based on a combined study of zircon U–Pb dating and CL imaging, petrology and C–O isotopes, the mid-Neoproterozoic limestone with the Triassic metamorphism are found in the Jiaobei terrane. It appears that the protolith of the Fenzishan marbles is the impure limestone that was deposited in the mid-Neoproterozoic rift basin of SCB continental margin. The positive $\delta^{13}C$ values for the limestone would probably form prior to the Sturtian glaciation. Therefore, the Fenzishan marbles geotectonically belong to the South China Block, corresponding to the sedimentary cover along the northern edge of South China Block. But it was detached from the Precambrian basement during the Triassic continent subduction, with a tectonic thrust for tens of kilometers over the southern margin of the North China Block. As a result, the marbles in affinity to the South China Block unusually occur overlying the basement of the North China Block.

Acknowledgments

This study was funded by grants from the Chinese Academy of Sciences (KZCX3-SW-141) and the Natural Science Foundation of China (40334036). Thank are due to Prof. D.-Y. Liu and Prof. Y.-S. Wan as well as Dr. Y.-B. Wang and Dr. Y.-R. Shi for their assistances with zircon SHRIMP U–Pb dating, to Prof. J.-X. Zhou and Mr. Z.-Y. Chen for their assistances with CL imaging, to Mr. M.-C. Song and Mr. X.-D. Zhang for their assistance with field trip. Comments by two anonymous reviewers greatly help improvements of the manuscript presentation.

References

Al-Aasm, I.S., Taylor, B.E., South, B., 1990. Stable isotope analysis of multiple carbonate samples using selective acid extraction. Chem. Geol. 80, 119–125.

Ames, L., Zhou, G.-Z., Xiong, B.-C., 1996. Geochronology and isotopic character of ultrahigh-pressure metamorphism with implications for collision of the Sino-Korean and Yangtze cratons, central China. Tectonics 15, 472–489.

An, Y.-H., 1990. A new division of the metamorphosed strata in the Jiaodong region: an account on the newly delimited Jiaodong Group and Jingshan Group. Shandong Geol. 6 (1), 97–103 (in Chinese with English abstract).

Boulvais, P., Fourcade, S., Gruau, G., Moine, B., Cuney, M., 1998. Persistence of pre-metamorphic C and O isotopic signatures in marbles subject to Pan-African granulite-facies metamorphism and U–Th mineralization (Tranomaro Southeast Madagascar). Chem. Geol. 150, 247–262.

Boulvais, P., Fourcade, S., Moine, B., Gruau, G., Cuney, M., 2000. Rare-earth elements distribution in granulite-facies marbles: a witness of fluid–rock interaction. Lithos 53, 117–126.

Bucher, K., Frey, M., 2002. Petrogenesis of Metamorphic Rocks, seventh ed. Springer-Verlag, Berlin Heidelberg, 341 pp.

Chu, X.L., Todt, W., Zhang, Q.R., Chen, F.K., Huang, J., 2005. U–Pb zircon age for the Nanhua-Sinian boundary. Chin. Sci. Bull. 50, 716–718.

Compston, W., Williams, I.S., Kirschvink, J.L., 1992. Zircon U–Pb ages for the Early Cambrian time-scale. J. Geol. Soc. Lond. 149, 171–184.

Condon, D., Zhu, M.Y., Bowring, S., Wang, W., Yang, A.H., Jin, Y.G., 2005. U–Pb ages from the Neoproterozoic Doushantou Formation, China. Science 308, 95–98.

Cong, B.-L., 1996. Ultrahigh-Pressure Metamorphic Rocks in the Dabie-Sulu Region of China. Science Press, Beijing, 224 pp.

Cong, B.-L., Wang, Q.-C., 1999. The Dabie-Sulu UHP rocks belt: review and prospect. Chin. Sci. Bull. 44, 1074–1085.

Eiler, J.M., Farley, K.A., Valley, J.W., Hoffman, A.W., Stolper, E.M., 1996. Oxygen isotope constrains on the sources of Hawaiian volcanism. Earth Planet. Sci. Lett. 120, 247–263.

Ellis, M., 1988. Lithospheric strength in compression: initiation of subduction, flake tectonics, foreland migration of thrusting, and an origin of displaced terranes. J. Geol. 96, 91–100.

Evans, D.A.D., Li, Z.X., Kirschvink, J.L., Wingate, T.D., 2000. A high-quality mid-Neoproterozoic paleomagnetic pole from South China, with implications for ice ages and the breakup configuration of Rodinia. Precambrian Res. 100, 313–334.

Fanning, C., Link, P.K., 2004. U–Pb SHRIMP ages of Neoproterozoic (Sturtian) glaciogenic Pocatello Formation, southeastern Idaho. Geology 32, 881–884.

Faure, M., Lin, W., Breton, N.L., 2001. Where is the North China–South China block boundary in eastern China? Geology 29, 119–122.

Faure, M., Breton, N.L., Lin, W., Monié, P., 2002. Where is the North China–South China block boundary in eastern China? Geology 30, 668 (reply).

Faure, M., Lin, W., Monié, P., Breton, N.L., Poussineau, S., Panis, D., Deloule, E., 2003. Exhumation tectonics of the ultrahigh-pressure metamorphic rocks in the Qinling orogen in east China: new petrological-structural-radiometric insights from the Shandong Peninsula. Tectonics 22, 1018–1040.

Fedo, C.M., Sircombe, K.N., Rainbird, R.H., 2003. Detrital zircon analysis of the sedimentary record. Zircon. Rev. Mineral. Geochem. 53, 277–303.

Fölling, P.G., Zartman, R.E., Frimmel, H.E., 2000. A novel approach to double-spike Pb–Pb dating of carbonate rocks: examples from Neoproterozoic sequences in southern Africa. Chem. Geol. 171, 97–122.

Guerrera, K., Peacock, S.M., Knauth, L.P., 1997. Large ^{18}O and ^{13}C depletion in greenschist facies carbonate rocks, western Arizona. Geology 25, 943–946.

Hacker, B., Ratschbacher, L., Webb, L., 1998. U/Pb zircon ages constrain the architecture of the ultrahigh-pressure Qinling-Dabie Orogen, China. Earth Planet. Sci. Lett. 161, 215–230.

Hoefs, J., 2004. Stable Isotope Geochemistry, fifth ed. Springer-Verlag, Heidelberg, 244 pp.

Hoffman, P.F., Kaufman, A.J., Halverson, G.P., Shrag, D.P., 1998. A Neoproterozoic Snowball Earth. Science 281, 1342–1346.

Hoffman, P.F., Schrag, D.P., 2002. The snowball Earth hypothesis: testing the limits of global change. Terra Nova 14, 129–155.

Hoffmann, K.H., Condon, D.J., Bowring, S.A., Crowley, J.L., 2004. U–Pb zircon date from the Neoproterozoic Ghaub Formation, Namibia: constraints on Marinoan glaciation. Geology 32, 817–820.

Holness, M.B., Bickle, M.J., Graham, C.M., 1991. On the kinetics of textural equilibration in forsterite marbles. Contrib. Mineral. Petrol. 108, 356–367.

Hoskin, P.W.O., Schaltegger, U., 2003. The compositions of zircon and igneous and metamorphic petrogenesis. Rev. Mineral. Geochem. 53, 27–55.

Jahn, B.-m., 1988. Pb–Pb dating of young marbles from Taiwan. Nature 332, 429–432.

Jahn, B.-m., Bertrand-Sarfati, J., Morin, N., Mace, J., 1990. Direct dating of stromatolitic carbonates from the Schmidtsdrif Formation (Transvaal Dolomite), South Africa, with implications on the age of the Ventersdorp Supergroup. Geology 18, 1211–1214.

Jahn, B.-m., Cuvellier, H., 1994. Pb–Pb and U–Pb geochronology of carbonate rocks: an assessment. Chem. Geol. 115, 125–151.

Kennedy, M.J., Runnegar, B., Prave, A.R., 1998. Two or four Neoproterozoic glaciations? Geology 26, 1059–1063.

Lambert, I.B., Walter, M.R., Zang, W., Lu, S., Ma, G., 1987. Paleoenvironment and carbon isotope stratigraphy of Upper Proterozoic carbonates of the Yangtze Platform. Nature 325, 140–142.

Li, Z.-X., 1994. Collision between the North and South China blocks: a crustal-detachment model for suturing in the region east of the Tanlu fault. Geology 22, 739–742.

Li, S.-G., Jagoutz, E., Lo, C.-H., Chen, Y.-Z., Li, Q.-L., Xiao, Y.-L., 1999. Sm/Nd, Rb/Sr and $^{40}Ar/^{39}Ar$ isotopic systematics of the ultrahigh-pressure metamorphic rocks in the Dabie-Sulu belt, Central China: a retrospective view. Intern. Geol. Rev. 41, 1114–1124.

Li, X.-H., 1997. Geochemistry of the Longsheng ophiolite from the southern margin of Yangtze Craton, SE China. Geochem. J. 31, 323–337.

Li, X.-H., Li, Z.-X., Ge, W.-C., Zhou, H.-W., Li, W.-X., Liu, Y., Wingate, M.T.D., 2003. Neoproterozoic granitoids in South China: crustal melting above a mantle plume at ca. 825 Ma? Precambrian Res. 122, 45–83.

Li, X.-P., Zheng, Y.-F., Wu, Y.-B., Chen, F.-K., Gong, B., Li, Y.-L., 2004. Low-T eclogite in the Dabie terrane of China: petrological and isotopic constrains on fluid activity and radiometric dating. Contrib. Mineral. Petrol. 148, 443–470.

Lin, S.F., van Staal, C.R., Dube, B., 1994. Promontory–promontory collision in the Canadian Appalachians. Geology 22, 897–900.

Lin, W.-W., Zhao, Y.-M., Zhao, G.-H., Xu, Y., Zhao, W.-G., 1998. Structure of Jingshan Group and the study on gold-bearing of Yetou Formation. Shandong Geol. 14, 42–49 (in Chinese with English abstract).

Liou, J.G., Zhang, R.-Y., Eide, E.A., Wang, X.-M., Ernst, W.G., Maruyama, S., 1996. Metamorphism and tectonics of high-pressure and ultra-high-pressure belts in the Dabie-Sulu region, China. In: Harrison, M.T., Yin, A. (Eds.), The Tectonics of Asia. Cambridge University Press, Cambridge, pp. 300–344.

Lu, S.N., 1998. Geochronology and Sm–Nd isotopic geochemistry of Precambrian crystalline basement in eastern Shandong province. Earth Sci. Front. 5, 275–283 (in Chinese with English abstract).

Ludwig, K.R., 2001. Users Manual for Isoplot/Ex (rev. 2.49): A Geochronological Toolkit for Microsoft Excel. Berkeley Geochronology Center, Special Publication, No. 1a, 55 pp.

Ma, G.G., Lee, H., Zhang, Z., 1984. An investigation of the age limits of the Sinian system in South China. Bull. Yichang Inst. Geol. Miner. Res. 8, 1–29 (in Chinese with English abstract).

McCrea, J.M., 1950. On the isotopic chemistry of carbonates and a paleotemperature scale. J. Chem. Phys. 18, 849–857.

Melezhik, V.A., Roberts, D., Fallick, A.E., Gorokhov, I.M., Kusnetzov, A.B., 2005. Geochemical preservation potential of high-grade calcite marble versus dolomite marble: implication for isotope chemostratigraphy. Chem. Geol. 216, 203–224.

Moorbath, S., Taylor, P.N., Orpen, J.L., Treloar, P., Wilson, J.F., 1987. First direct radiometric dating of Archaean stromatolite limestone. Nature 326, 865–867.

O'Neil, J.R., 1987. Preservation of H, C and O isotopic ratios in the low temperature environment. In: Kyser, T.K. (Ed.), Short Course in Stable Isotope Geochemistry of Low Temperature Fluids, vol. 13. MAC Short Course Handbook, pp. 85–128.

Oxburgh, E.R., 1972. Flake tectonics and continental collision. Nature 239, 202–204.

Prave, A.R., 1999. Two diamictites, two cap carbonates, two $\delta^{13}C$ excursions, two rifts: the Neoproterozoic Kingston Peak Formation, Death Valley, California. Geology 27, 339–342.

Price, R.A., 1986. The southeastern Canadian Cordillera Thrust faulting, tectonic wedge, and delamination of the lithosphere. J. Struct. Geol. 8, 239–254.

Ramsey, M.H., Potts, P.J., Webb, P.C., Watkins, P., Watson, J.S., Coles, B.J., 1995. An objective assessment of analytical method precision: comparison of ICP-AES and XRF for the analysis of silicate rocks. Chem. Geol. 124, 1–19.

Romanek, C.S., Grossman, E.L., Morse, J.W., 1992. Carbon isotope fractionation in synthetic aragonite and calcite: effects of temperature and precipitation rate. Geochim. Cosmochim. Acta 56, 419–430.

Rubatto, D., Gebauer, G., Compagnoni, R., 1999. Dating of eclogite-facies zircons: the age of Alpine metamorphism in the Sesia-Lanzo Zone (Western Alps). Earth Planet. Sci. Lett. 167, 141–158.

Rumble, D., Wang, Q.-C., Zhang, R.-Y., 2000. Stable isotope geochemistry of marbles from the coesite UHP terrains of Dabieshan and Sulu, China. Lithos 52, 79–95.

Shandong (Shandong Bureau of Geology and Mineral Resources), 1991. Regional Geology of Shandong Province. Geological Publishing House, Beijing, 595 pp. (in Chinese with English abstract).

Shen, Y.-N., 2002. C-isotope variations and paleoceanographic changes during the late Neoproterozoic on the Yangtze Plateform, China. Precambrian Res. 113, 121–133.

Stacey, J.S., Kramers, J.D., 1975. Approximation of terrestrial lead isotope evolution by a two-stage model. Earth Planet. Sci. Lett. 26, 207–221.

Stockmal, G.S., Colman-Sadd, S.P., Keen, C.E., Marillier, F., O'Brien, S.J., Quinlan, G.M., 1990. Deep Seismic structure and plate tectonic evolution of the Canadian Appalachians. Tectonics 9, 45–62.

Sun, S.-s., McDonough, W.F., 1989. Chemical and isotopic systematics of oceanic basalt: implications for mantle composition and process. In: Saunders, A.D., Norry, M.J. (Eds.), Magmatism in the Ocean Basins. Geological Society Special Publication, No. 42, pp. 313–345.

Tang, J., Zheng, Y.-F., Wu, Y.-B., Zha, X.-P., Zhou, J.-B., 2004. Zircon U–Pb ages and oxygen isotopes of metamorphic rocks in the western part of the Shandong Peninsula. Acta Petrol. Sin. 20, 1063–1086 (in Chinese with English abstract).

Taylor, P.N., Kalsbeek, F., 1990. Dating of metamorphism of Precambrian marbles: examples from Proterozoic mobile belts in Greenland. Chem. Geol. 86, 21–28.

Turner, J.V., 1982. Kinetic fractionation of carbon-13 during calcium carbonate precipitation. Goechim. Cosmochim. Acta 46, 1183–1191.

Valley, J.W., 1986. Stable isotope geochemistry of metamorphic rocks. Rev. Miner. 16, 445–489.

Valley, J.W., Kitchen, N.E., Kohn, M.J., Niendorf, C.R., Spicuzza, M.J., 1995. A garnet standard for oxygen isotope ratio: strategies for high precision and accuracy with laser heating. Geochim. Cosmochim. Acta 59, 5223–5231.

Vavra, G., Schmid, R., Gebauer, D., 1999. Internal morphology, habit and U–Th–Pb microanalysis of amphibolite to granulite facies zircon: geochronology of the Ivren Zone (Southern Alps). Contrib. Mineral. Petrol. 134, 380–404.

Wallis, S., Enami, M., Banno, S., 1999. The Sulu UHP Terrane: a review of the petrology and structural geology. Intern. Geol. Rev. 41, 906–920.

Wan, T.-F., Zeng, H.-L., 2002. The distinctive characteristics of the Sino-Korean and the Yangtze plates. J. Asian Earth Sci. 20, 881–888.

Wang, D.H., Lin, R.S., 1991. Metamorphic characterization of the Lower Proterozoic Jinshan Group in the Pingdu area, Shangdong province. Shandong Geol. 7 (2), 1–16 (in Chinese).

Wang, P.-C., 1995. Relationships between the Jinshan Group and the Fenzishan Group in the Jiaobei area. Regional Geol. Chin. 1, 15–20 (in Chinese with English abstract).

Wang, P.-C., An, Y.-H., 1996. Main achievement and progress of the basic geological research over last ten years in eastern Shandong region. Shandong Geol. 12, 8–23 (in Chinese with English abstract).

Wang, Q.-C., Cong, B.-L., 1998. Tectonic framework of ultrahigh pressure metamorphic belt in Dabieshan. Acta Petrol. Sin. 14, 481–492 (in Chinese with English abstract).

Wang, Z.S., Rasbury, E.T., Hanson, G.N., Meyers, W.J., 1998. Using the U–Pb system of calcretes to date the time of sedimentation of clastic sedimentary rocks. Geochim. Cosmochim. Acta 62, 2823–2835.

Wang, J., Li, Z.-X., 2003. History of Neoproterozoic rift basins in South China: implications for Rodinia break-up. Precambr. Res. 122, 141–158.

Wickham, S.M., Peters, M.T., 1993. High $\delta^{13}C$ Neoproterozoic carbonate rocks in western North America. Geology 21, 165–168.

Williams, I.S., 1998. U–Th–Pb geochronology by ion microprobe. In: Applications of Microanalytical Technique to Understanding Mineralizing Process. Rev. Econ. Geol. 7, 1–35.

Woodhead, J.D., Hergt, J.M., 1997. Application of the “double spike” technique to Pb-isotope geochronology. Chem. Geol. 138, 311–321.

Wu, Y.-B., Zheng, Y.-F., Zhou, J.-B., 2004. Neoproterozoic granitoid in northwest Sulu and its bearing on the North China-South China Blocks boundary in east China. Geophys. Res. Lett. 31, L07616, doi: 10.1029/2004GL019785.

Yang, W.-C., 2002. Geophysical profiling across the Sulu ultra-high-pressure metamorphic belt, eastern China. Tectonophysics 354, 277–288.

Yin, C.Y., Liu, D.Y., Gao, L.Z., Xing, Y.S., Jian, P., Shi, Y.R., 2003. The lower boundary age of the Nanhua System and the Gucheng glacial stage: evidence from SHRIMP II dating. Chin. Sci. Bull. 48, 1657–1662.

Zhai, M.-G., Cong, B.-L., Guo, J.-H., Liu, W.-J., Li, Y.-G., Wang, Q.-C., 2000. Sm–Nd geochronology and petrography of garnet pyroxene granulites in the northern Sulu region of China and their geotectonic implication. Lithos 52, 23–33.

Zhai, M.-G., 2002. Where is the North China–South China block boundary in eastern China? Geology 30, 667 (comment).

Zhang, Q.R., Piper, J.D.A., 1997. Palaeomagnetic study of Neoproterozoic glacial rocks of the Yangzi Block: palaeolatitude and configuration of South China in the late Proterozoic Supercontinent. Precambrian Res. 85, 173–199.

Zhang, S.H., Jiang, G.Q., Zhang, J.M., Kennedy, M.J., Christie-Blick, N., 2005. U–Pb sentitive high-resolution ion microprobe ages from the Doushantou Formation in south China: constraints on late Neoproterozoic glaciations. Geology 33, 473–476.

Zhao, G.-C., Wilde, S.A., Cawood, P.A., Sun, M., 2001. Archean blocks and their boundaries in the North China Craton: lithological, geochemical, structural and *P–T* path constraints and tectonic evolution. Precambrian Res. 107, 45–73.

Zhao, Y.-Y., Hu, S.-X., Xu, B., Lu, B., Ji, H.-Z., 1995. Problems on Precambrian strata of the Jiaobei terrane, Shandong province. Regional Geol. Chin. 3, 272–279 (in Chinese with English abstract).

Zhao, Z.-F., Zheng, Y.-F., Wei, C.-S., Wu, Y.-B., 2004. Zircon isotope evidence for recycling of subducted continental crust in post-collisional granitoids from the Dabie terrane in China. Geophys. Res. Lett. 31, L22602, doi:10.1029/2004GL021061.

Zhao, Z.-F., Zheng, Y.-F., Wei, C.-S., Wu, Y.-B., Chen, F.-K., Jahn, B.-m., 2005. Zircon U–Pb age, element and C–O isotope geochemistry of post-collisional mafic-ultramafic rocks from the Dabie orogen in east-central China. Lithos 83, 1–28.

Zheng, Y.-F., 1993a. Calculation of oxygen isotope fractionation in anhydrous silicate minerals. Geochim. Cosmochim. Acta 5, 1079–1091.

Zheng, Y.-F., 1993b. Calculation of oxygen isotope fractionation in hydroxyl-bearing silicate. Earth Planet. Sci. Lett. 120, 247–263.

Zheng, Y.-F., Fu, B., Gong, B., Wang, Z.-R., 1998. Carbon isotope anomaly in marbles associated with eclogites from the Dabie Mountains in China. J. Geol. 106, 97–104.

Zheng, Y.-F., 1999. Oxygen isotope fractionation in carbonate and sulfate minerals. Geochem. J. 33, 109–126.

Zheng, Y.-F., Wang, Z.-R., Li, S.-G., Zhao, Z.-F., 2002. Oxygen isotope equilibrium between eclogite minerals and its constraints on mineral Sm–Nd chronometer. Geochim. Cosmochim. Acta 66, 625–634.

Zheng, Y.-F., Fu, B., Gong, B., Li, L., 2003. Stable isotope geochemistry of ultrahigh pressure metamorphic rocks from the Dabie-Sulu orogen in China: implications for geodynamics and fluid regime. Earth Sci. Rev. 62, 105–161.

Zheng, Y.-F., Wu, Y.-B., Chen, F.-K., Gong, B., Zhao, Z.-F., 2004. Zircon U–Pb and oxygen isotope evidence for a large-scale ^{18}O depletion event in igneous rocks during the Neoproterozoic. Geochim. Cosmochim. Acta 68, 4145–4165.

Zheng, Y.-F., Zhou, J.-B., Wu, Y.-B., Xie, Z., 2005. Low-grade metamorphic rocks in the Dabie-Sulu orogenic belt: A passive-margin accretionary wedge deformed during continent subduction. Intern. Geol. Rev. 47, 851–871.

Zhou, G.-T., Zheng, Y.-F., 2001. Chemical synthesis of $CaCO_3$ minerals at low temperatures and implication for mechanism of polymorphic transition. N. Jb. Miner. Abh. 176, 323–343.

Zhou, X.-W., Dong, Y.-S., Wei, C.-D., 2001. The genesis and evolution of the metamorphic minerals of Khodalite series in Nanshu district of Shandong Province. J. Changchun Univ. Sci. Technol. 31 (2), 116–121 (in Chinese with English abstract).

Zhou, G.-T., Zheng, Y.-F., 2002. Kinetic mechanism of oxygen isotope disequilibrium in precipitated witherite and aragonite at low temperatures: an experimental study. Geochim. Cosmochim. Acta 66, 63–71.

Zhou, G.-T., Zheng, Y.-F., 2003. An experimental study of oxygen isotope fractionation between inorganically precipitated aragonite and water at low temperatures. Geochim. Cosmochim. Acta 67, 387–399.

Zhou, C.M., Tucker, R., Xiao, S.H., Peng, Z.X., Chen, Z., 2004a. New constraints on the ages of Neoproterozoic glaciations in south China. Geology 32, 437–440.

Zhou, X.-W., Wei, C.-J., Geng, Y.-S., Zheng, L.-F., 2004b. Discovery and implications of the high-pressure pelitic granulites from the Jiaobei massif. Chin. Sci. Bull. 49, 1942–1948.

Zhou, G.-T., Zheng, Y.-F., 2005. Effect of polymorphic transition on oxygen isotope fractionation between aragonite, calcite and water: a low-temperature experimental study. Am. Miner. 90, 1121–1130.